AD-A080 116 NATIONAL AERONAUTICS AND SPACE ADMINISTRATION CLEVEL--ETC F/G 20/11
DIRECT INTEGRATION OF TRANSIENT ROTOR DYNAMICS.(U)
JAN 80 A F KASCAK

UNCLASSIFIED NASA-E-101 NASA-TP-1597 NL

| OF |
AD
A080116

END
DATE
FILMED
3-80
DDC

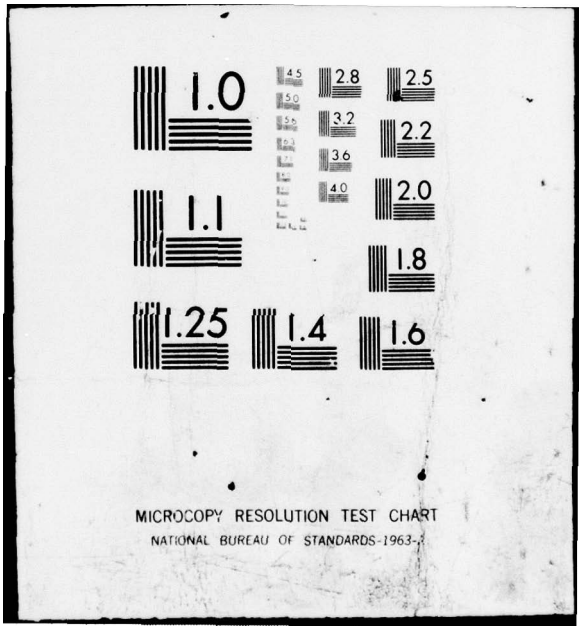
1.0
1.1
1.25
1.4
1.6
1.8
2.0
2.2
2.5
2.8
3.2
3.6
4.0
4.5
5.0
MICROCOPY RESOLUTION TEST CHART
NATIONAL BUREAU OF STANDARDS-1963-A

NASA
Technical Paper 1597

AVRADCOM
Technical Report 79-42

Direct Integration of Transient Rotor Dynamics

Albert F. Kascak

JANUARY 1980

NASA

NASA
Technical Paper 1597

AVRADCOM
Technical Report 79-42

Direct Integration of Transient Rotor Dynamics

Albert F. Kascak
Propulsion Laboratory, AVRADCOM Research and Technology Laboratories
Lewis Research Center
Cleveland, Ohio

National Aeronautics
and Space Administration

Scientific and Technical Information Office

1980

SUMMARY

A study was conducted to develop an implicit method for integrating the equations of motion of a lumped-mass model of a rotor bearing system. The approach was, first, to use a Nordsieck-like numerical integration directly on the second-order equations of motion and, second, to assume that the forces and torques on the rotor are functions of the position and velocity at the point of application and its nearest axial neighbors. This allows the variables to be arranged so that the Jacobian of the set of nonlinear equations is block tridiagonal. Therefore the computational time is proportional to the number of elements in the rotor dynamics model rather than to the cube of the number. Numerical stability was demonstrated for any linearized homogeneous mode.

To decrease computational time, a closed-form solution to the short-bearing theory was derived for a damper with arbitrary motion. Explicit results were presented for no cavitation and for full cavitation.

The vast amount of data generated by the computer code was displayed in a motion picture showing an oblique view of the rotor bearing system. The motion of the rotor could be easily interpreted.

An example problem of a rotor accelerating through three critical speeds with 19 mass elements in the rotor dynamics model took 0.7 second of central processing unit time per time step on an IBM 360-67 computer in a time-sharing mode. The mode shapes at the first and third critical speeds were similar to the predicted mode shapes and occurred at the predicted speed. Because of the unbalance distribution, the second mode was not excited. Above the third critical speed the rotor bearing system operated as a self-centering device. This was also observed experimentally.

The computer code, for the first time, allows us to look at a complex rotor bearing system with nonlinear transients and displays the vast amount of results in an easily understood motion-picture format. A 10-minute 16-millimeter, color, sound motion-picture supplement is available on loan.

INTRODUCTION

Nonlinear transients that are important in flexible, rotating equipment are difficult to analyze. Such things as blade tip rubs, spline friction, and squeeze-film dampers are difficult to predict with a linear model. Some of the transients that are important are locked rotor starts, blade loss, and rapid deceleration due to bearing failures.

There are two basic methods for studying transient rotor dynamics. The first method is the modal method (refs. 1 and 2). It is best suited to linear rotor bearing systems running at a constant speed. The second method is the direct integration of the equations of motion. It can be applied easily to nonlinear systems that are varying in speed. The problem with the direct method is that it is limited by either computer running time or numerical stability.

The equations of motion for rotor dynamics can be integrated directly in either of two ways, explicit or implicit integration. The explicit integration method solves the equations of motion at the present time for higher order derivatives and then extrapolates the displacements and velocities with a Taylor series to the advanced time (ref. 3). The implicit method solves the equations of motion (implicitly) at the advanced time step for

the displacements and velocities, such that an extrapolation backward in time gives the previous results.

The explicit method tends to be unstable when the product of the critical frequency (for any mode numerically possible) and the time step is large (ref. 4). Since the highest frequency is related to the square of the number of elements in the rotor dynamics model, the computational time will be related to the square of the number of elements. Approximately five or six elements seems to be a practical limit to the explicit method (ref. 2); that is, it can only be applied to simple assemblies.

In contrast to the explicit method, the implicit method tends to be stable for large time steps (ref. 5); but it requires the solution of a large number of nonlinear simultaneous equations at each time step. For every element in the rotor dynamics model there are four degrees of freedom. For each degree of freedom there is an associated displacement and velocity. Therefore the total number of nonlinear equations to be solved at each time step is eight times the number of elements in the rotor dynamics model. The number of computations necessary to solve these equations is proportional to the cube of the number of equations. Therefore the computing time is proportional to the cube of the number of elements.

This study was conducted to develop an implicit method for integrating the equations of motion in a reasonable amount of computing time. The approach is, first, to use a Nordsieck-like numerical integration directly on the second-order equations of motion[1] and, second, to assume that the forces and torques on the rotor are functions of the position and velocity of the point where the force or torque is applied and its nearest axial neighbors. This allows the variables to be arranged so that the Jacobian of the set of nonlinear equations is block tridiagonal. The computing time is proportional to the number of elements in the rotor dynamics model rather than to the cube of the number of elements.

Besides the problems associated with integrating the equations of motion, there is a problem of describing the nonlinear damper force at each instant of time for an arbitrary orbit. In the past this was done by numerically integrating the Reynolds equation around the damper (ref. 6). This required a considerable amount of computing time. As an aside, a closed-form solution to the short-bearing theory was derived for a damper with arbitrary motion.

SYMBOLS

A	coefficients used in partial-fraction expansion
a	property of shaft between mass stations defined in eq. (18a)
b	property of shaft between mass stations defined in eq. (18b)
C	radial clearance
c	property of shaft between mass stations defined in eq. (18c)
D	diameter

[1]This method of numerical integration was developed by Frank J. Zeleznik of the Lewis Research Center. For a set of first-order equations, it reduces to Gear's method.

E	modulus of elasticity
F	force
G	torque
h	clearance in direction $\hat{n}$
I	moment of inertia
j	index
k	index
L	axial length between mass stations
m	mass of a rotor segment
N	number of rotor segments
n	radial direction at angle θ
O	order of error in Taylor series
P	pressure
q	order of Taylor series
r	radial displacement
S	stability matrix
s_{kj}	element of S
t	time
Δt	time step
u	defined in eq. (5)
V	nondimensional velocity of journal in rotating coordinates
x	real part of radial displacement
y	imaginary part of radial displacement
Z	independent variable
z	axial coordinate
α_k	given set of constants

Γ	angle defined in eq. (43)
ϵ	eccentricity ratio
ζ	damping ratio
θ	circumferential angle
λ	eigenvalue of stability matrix
μ	viscosity
ω	frequency

Subscripts:

B	bearing
J	journal
P	polar
T	transverse
$\pm$	associated with nearest axial neighbor or root of eq. (45)
0	start of integration
1	end of integration

Superscripts:

$(\dot{})$	time derivative
$()'$	axial derivative
$(\bar{})$	average or conjugate
(k)	k^{th} time derivative
$\rightarrow$	vector
$\hat{}$	unit vector

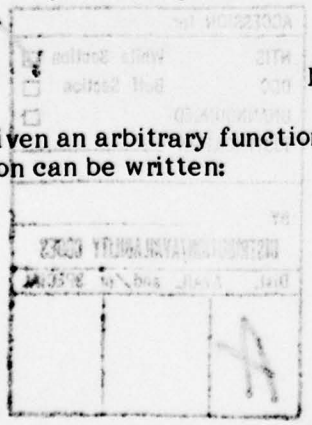

NUMERICAL INTEGRATION

Given an arbitrary function $Z_k(t)$ whose derivatives exist, $Z_k^{(j)}(t)$, a Taylor series expansion can be written:

$$z_k(t + \Delta t) = \sum_{j=0}^{q-k} \frac{(\Delta t)^j}{j!} z_k^{(j)}(t) + O_{q-k} \tag{1}$$

with Lagrange's remainder of order O_{q-k}. If the arbitrary function is chosen as

$$z_k = \frac{(\Delta t)^k}{k!} r^{(k)} \tag{2}$$

the Taylor series for this function becomes

$$z_k(t + \Delta t) = \sum_{j=0}^{q} \binom{j}{k} z_j(t) + O_q \tag{3}$$

where the binomial coefficients are defined as

$$\binom{j}{k} = \begin{cases} \dfrac{j!}{k!(j-k)!} & \text{for } j \geq k \\ 0 & \text{for } j < k \end{cases} \tag{4}$$

If the form of the remainder is chosen as

$$O_q = \alpha_k u \tag{5}$$

the Taylor series becomes

$$z_k(t + \Delta t) = \sum_{j=0}^{q} \binom{j}{k} z_j(t) + \alpha_k u \tag{6}$$

where α_k is a given set of constants and u can be determined from the equation of motion at the advanced time. The equation of motion at the advanced time is

$$\sum F(r, \dot{r}, \ddot{r}, t + \Delta t) = 0 \tag{7}$$

From the definition of z, the various derivatives become

$$r^{(k)} = \frac{k!}{(\Delta t)^k} z_k \tag{8}$$

Substituting for the various derivatives into the equation of motion and knowing the values at the previous time result in the equation of motion being a function of

$$\sum F(u,\ t + \Delta t) = 0 \tag{9}$$

This equation can be solved for u and, from this value of u, the remainder can be used as an error estimate to control the time step.

NUMERICAL STABILITY

The analysis of the stability of the numerical integration technique assumes a model of a rotor bearing system that is linearized at some instant of time. The homogeneous equation of motion for any mode is

$$\ddot{r} + 2\omega\zeta\dot{r} + \omega^2 r = 0 \tag{10}$$

where ω is the natural frequency and ζ is the damping ratio for the mode. For every mode that is numerically possible, with nonnegative damping ratio, the amplitude must either remain constant or decay in time. The numerical integration is defined as unstable if the amplitude grows in time.

From the definition of z the modal equation becomes

$$2Z_2 + 2\omega\,\Delta t\ \zeta Z_1 + (\omega\ \Delta t)^2 Z_0 = 0 \tag{11}$$

Substituting the Taylor series into the modal equation at the advanced time results in

$$u = -\sum_{j=0}^{q} \left[\frac{j(j-1) + 2j\omega\,\Delta t\ \zeta + (\omega\ \Delta t)^2}{2\alpha_2 + 2\alpha_1\omega\,\Delta t\ \zeta + \alpha_0(\omega\ \Delta t)^2}\right] Z_j(t) \tag{12}$$

For this value of u, the Taylor series expresses the solution at the advanced time in terms of the solution at the present time as

$$Z_k(t + \Delta t) = \sum_{j=0}^{q} \left\{\binom{j}{k} - \frac{\alpha_k\left[j(j-1) + 2j\omega\,\Delta t\ \zeta + (\omega\ \Delta t)^2\right]}{\left[2\alpha_2 + 2\alpha_1\omega\,\Delta t\ \zeta + \alpha_0(\omega\ \Delta t)^2\right]}\right\} Z_j(t) \tag{13}$$

Defining the matrix element s_{kj} to be

$$s_{kj} = \binom{j}{k} - \frac{\alpha_k\left[j(j-1) + 2j\omega\,\Delta t\ \zeta + (\omega\ \Delta t)^2\right]}{\left[2\alpha_2 + 2\alpha_1\omega\,\Delta t\ \zeta + \alpha_0(\omega\ \Delta t)^2\right]} \tag{14}$$

and the q-dimension vector $\vec{Z}$ gives the eigenvalue equation as

$$S\vec{Z} = \lambda\vec{Z} \tag{15}$$

If the $|\lambda| > 1$, the amplitude grows and the method is numerically unstable. For $q = 2$, the given α's are $\alpha_0 = 2$, $\alpha_1 = 3$, and $\alpha_2 = 1$. In the limit as $\omega \Delta t \to \infty$, the maximum $|\lambda| \to 0$. Therefore if the time step Δt is much larger than ω^{-1} for a mode, the amplitude of that mode will approach zero. If a mode is to have a nonzero amplitude, ωh must be small. In the limit as $\omega \Delta t \to 0$, the maximum $|\lambda| \to 1$. Therefore the method is numerically stable in the two limits.

EQUATIONS OF MOTION

A model of the shaft showing the complex number representation of the radial displacement r is shown in figure 1. The radial displacement is the distance between the shaft centerline and the axis of rotation. It can be represented by

$$r = x + iy \tag{16a}$$

where the real and imaginary axes are fixed in space perpendicular to the axis of rotation. The slope of the shaft along the axis of rotation is

$$r' = x' + iy' \tag{16b}$$

The position of the shaft is then described by r and r' at all the axial locations.

The lumped-mass model of a rotor divides the rotor into N segments. The mass and inertia of each segment are assumed to be concentrated at a point. These points are then assumed to be connected by massless elastic beams that model the stiffness of the rotor.

The equations of motion for the lumped-mass model were derived in reference 7. The sum of the forces $\sum F$ at a point, must be zero, where

$$\sum F = -m\ddot{r} + a_- r_- - (a_- + a_+)r + a_+ r_+ + b_- r'_- + (b_- - b_+)r' - b_+ r'_+ + F = 0 \tag{17a}$$

and the sum of the torques $\sum G$ about a point must be zero, where

$$\sum G = -I_T \ddot{r}' + i\omega I_p \dot{r}' - \dot{\omega} I_p r' - b_- r_- + (b_- - b_+)r + b_+ r_+ - c_- r'_- - 2(c_- + c_+)r' - c_+ r'_+ + G \tag{17b}$$

The + or - refer to the next or previous axial location; and a, b, and c are properties of the shaft between these locations:

$$a = 12EI/L^3 \tag{18a}$$

$$b = 6EI/L^2 \tag{18b}$$

$$c = 2EI/L \tag{18c}$$

If the nonlinear force F and the nonlinear torque G are functions of displacements and velocities of the point and its nearest neighbors, the $\sum F$ and $\sum G$ are functions of the displacements and velocities of the point and its nearest neighbors. If the Taylor series of the numerical integration technique is substituted into the equations of motion for the acceleration, velocity, and displacement, the form of the equations of motion becomes

$$0 = \sum F(u_-, u, u_+, u'_-, u', u'_+) \tag{19a}$$

$$0 = \sum G(u_-, u, u_+, u'_-, u', u'_+) \tag{19b}$$

These equations form a set of 2N complex nonlinear equations in 2N unknowns. These equations are solved by rewriting them as 4N real equations in 4N real unknowns and then using a Newton-Raphson iterative technique to obtain a numerical solution. The Newton-Raphson technique assumes a solution, linearizes the equations about that solution, and then solves the linear set of equations for a correction to the assumed solution. The form of the equations of motion results in the linear set of equations being block tridiagonal (fig. 2). The block-tridiagonal form allows the set of equations to be solved in a very efficient manner. The computing time is proportional to N rather than to N^3 as in the general method.

SQUEEZE-FILM DAMPER BEARING

The configuration of the squeeze-film damper is shown in figure 3. The same configuration can be used to analyze journal bearings where the journal and the bearing are allowed to rotate. If ω_J is the rotational speed of the journal and ω_B is the rotational speed of the bearing, the average rotational speed is

$$\bar{\omega} = \frac{1}{2}(\omega_B + \omega_J) \tag{20}$$

For a damper this average rotational speed would be zero.

If C is the radial clearance and $\vec{r}$ is the displacement of the journal center with respect to the bearing center, the clearance h in the direction $\hat{n}$ is

$$h = c - \vec{r} \cdot \hat{n} \tag{21}$$

If $\dot{\vec{r}}$ is the velocity of the journal,

$$\frac{\partial h}{\partial t} = -\dot{\vec{r}} \cdot \hat{n} \tag{22}$$

If $\hat{n}$ is at an angle θ,

$$\frac{\partial \hat{n}}{\partial \theta} = \hat{k} \times \hat{n} \tag{23}$$

where $\hat{k}$ is a unit vector along the axis of the damper bearing in the z-direction. If $\vec{\omega}$ is defined as

$$\vec{\omega} = \bar{\omega}\hat{k} \tag{24}$$

then

$$\bar{\omega} \frac{\partial h}{\partial \theta} = (\vec{\omega} \times \vec{r}) \cdot \hat{n} \tag{25}$$

The Reynolds equation for the short, plain damper journal bearing is presented in reference 6 as

$$\frac{\partial}{\partial z}\left(\frac{h^3}{12\mu}\frac{\partial P}{\partial Z}\right) = \bar{\omega}\frac{\partial h}{\partial \theta} + \frac{\partial h}{\partial t} \tag{26}$$

If the boundary conditions in the damper bearing are

$$P(0, \theta, t) = 0 \tag{27a}$$

$$P(L, \theta, t) = 0 \tag{27b}$$

and if h is not a function of z,

$$P = -\frac{6\mu z(L - z)}{h^3}(\vec{\omega} \times \vec{r} - \dot{\vec{r}}) \cdot \hat{n} \tag{28}$$

The eccentricity ratio is

$$\vec{\epsilon} = \frac{\vec{r}}{C} \tag{29}$$

so that

$$\dot{\vec{\epsilon}} = \frac{\dot{\vec{r}}}{C} \tag{30}$$

If $\vec{V}$ is defined as

$$\vec{V} = \dot{\vec{\varepsilon}} - \vec{\omega} \times \vec{\varepsilon} \tag{31}$$

$$P = \frac{6\mu z(L - z)}{C^2(1 - \vec{\varepsilon} \cdot \hat{n})} \vec{V} \cdot \hat{n} \tag{32}$$

The pressure is zero when $\hat{n}$ is perpendicular to $\vec{V}$, and the pressure is greater than zero when $\vec{V} \cdot \hat{n} > 0$.

The force on the journal due to the pressure in a segment of the film extending from θ_0 to θ_1 is

$$\vec{F} = -\frac{D}{2} \int_{\theta_0}^{\theta_1} \int_0^L P\hat{n} \, dz \, d\theta \tag{33}$$

This expression for the force can be integrated axially and becomes

$$\vec{F} = -\frac{\mu D L^3}{2C^2} \int_{\theta_0}^{\theta_1} \frac{(\vec{V} \cdot \hat{n})\hat{n}}{(1 - \vec{\varepsilon} \cdot \hat{n})^3} \, d\theta \tag{34}$$

The angular integral can be integrated by transforming the integral to the complex plane (fig. 4). Let $\vec{V}$ be in the real direction, $\vec{\varepsilon}$ be at an angle ϕ, and $\hat{n}$ be at an angle θ so that

$$V = |V| \tag{35a}$$

$$\varepsilon = |\varepsilon| e^{i\phi} \tag{35b}$$

$$n = e^{i\theta} \tag{35c}$$

Differentiating the expression for n yields

$$d\theta = -in^{-1} \, dn \tag{36}$$

and using the definition of the complex cosine yields

$$\vec{V} \cdot \hat{n} = \frac{V(n + n^{-1})}{2} \tag{37}$$

$$\vec{\varepsilon} \cdot \hat{n} = \frac{(n\bar{\varepsilon} + \varepsilon n^{-1})}{2} \tag{38}$$

The expression for the force becomes

$$F = -i\left(\frac{2\mu DL^3}{C^2}\right)V \oint \frac{n^2(n^2+1)dn}{(\bar{\varepsilon}n^2 - 2n + \varepsilon)^3} \tag{39}$$

where the integral is around the unit circle from n_0 to n_1, where

$$n_0 = e^{i\theta_0} \tag{40a}$$

$$n_1 = e^{i\theta_1} \tag{40b}$$

The pressure is zero at $n = \pm i$, and the pressure is greater than zero when $Re(n)$ is greater than zero.

For no cavitation the integral extends completely around the journal; and by using the theory of residues, the force becomes

$$F = 4\pi\left(\frac{\mu DL^3}{C^2}\right)\left(\frac{V}{\bar{\varepsilon}^3}\right)A_{-1} \tag{41}$$

For cavitation the integral extends from $-i$ to $+i$; and by using a partial-fraction technique, the force becomes

$$F = 4\left(\frac{\mu DL^3}{C^2}\right)\left(\frac{V}{\bar{\varepsilon}^3}\right)\left\{\Gamma A_- + \sum_{j=2}^{3}\left[\frac{(-n_+)^{j-2}A_{+j}}{(1+n_+^2)^{j-1}} + \frac{(-n_-)^{j-2}A_{-j}}{(1+n_-^2)^{j-1}}\right]\right\} \tag{42}$$

where Γ is defined as

$$\Gamma = \tan^{-1}\frac{\sqrt{1-|\varepsilon|^2}}{-Re(\varepsilon)} \tag{43}$$

and Γ is in the first or second quadrant. The partial-fraction expansion coefficients are

$$A_{\pm 3} = \frac{n_\pm^2(n_\pm^2+1)}{(n_\pm - n_\mp)^3} \tag{44a}$$

$$A_{\pm 2} = \frac{2n_{\pm}(2n_{\pm}^2 + 1)}{(n_{\pm} - n_{\mp})^3} - \frac{3A_{\pm 3}}{n_{\pm} - n_{\mp}} \tag{44b}$$

$$A_{\pm 1} = \frac{6n_{\pm}^2 + 1}{(n_{\pm} - n_{\mp})^3} - \frac{3A_{\pm 2}}{n_{\pm} - n_{\mp}} - \frac{3A_{\pm 3}}{(n_{\pm} - n_{\mp})^2} \tag{44c}$$

where the roots of the denominator of the force equation are

$$n_{\pm} = \left(\frac{1 \pm \sqrt{1 - |\epsilon|^2}}{|\epsilon|^2} \right) \epsilon \tag{45}$$

DISCUSSION OF EXAMPLE

The rotor bearing system described in reference 8 was used as the example problem. This rotor bearing system consisted of a shaft with three disks mounted on two axially preloaded ball bearings (fig. 5). The bearings were mounted in a squeeze-film damper journal, and the journal had a centering spring.

The first three critical speeds for the rotor bearing system without oil in the damper are shown in figure 6. All the modes are bent-shaft modes. The "classical" hierarchy only applies to stiff shafts; therefore, the classical mode shapes do not characterize the actual mode shapes. The first mode, about 7581 rpm, classically would be the cylindrical mode. But in this case, it has a large amount of bending outward near the shaft center. The second mode, about 9235 rpm, classically would be the conical mode. In this case, it has a slight amount of bending outward near the shaft ends. The third mode, about 11 248 rpm, classically would be the bending mode. In this case, it has a large amount of bending throughout the shaft.

Experimentally the rotor was accelerated from rest through the three critical speeds. The Lissajous patterns for the three disks were displayed on three side-by-side cathode ray tubes. A motion picture was taken of the CRT's plus a speed counter. The Lissajous patterns at the three critical speeds are shown on figures 7 to 9. The three critical speeds occurred at about the predicted speeds, and the Lissajous patterns corresponded to the three mode shapes.

The rotor bearing system was modeled by using 19 elements. The rotor was assumed to have a uniform, in-line unbalance, with a mass eccentricity of 0.00254 centimeter (1 mil). The equations of motion for this system were programed in FORTRAN IV on an IBM 360-67 computer in a time-sharing mode. The equations of motion were directly integrated by the implicit integration method, with a fixed time step of 0.12 millisecond. The transient analyzed was the rotor accelerated from rest through the three critical speeds. The rate of acceleration was 8727 rad/sec^2. Each time step took about 0.7 second of CPU time.

The output at each time step of the calculation was displayed on a CRT. The display showed an oblique view of the rotor bearing system, with the bearing centerline as the oblique axis. The transverse vibration is indicated by a series of dots. Each dot represents a

location of an element in the rotor dynamics model. The scale of the transverse vibration exaggerates the amplitude of the vibration. The display on the CRT was photographed at each time step. These photographs were then shown as a motion picture.

The computer-generated displays on the CRT at the first and third critical speeds and at a speed much greater than the third critical speed are shown in figures 10 to 12. The mode shapes at the first and third critical speeds were similar to the predicted mode shapes and occurred at the predicted speed. Because of the unbalance distribution, the second mode was not excited. The only indication of the second mode was a traveling wave superimposed on the first mode shape. This traveling wave decayed when the rotor went through the third critical speed. Above the third critical speed, the rotor bearing system operated as a self-centering device. The mass centerline coincided with the bearing centerline. Therefore, the rotor displacement was uniform and in line, with an amplitude of 0.00254 centimeter (1 mil).

In conclusion, this computer code for the first time allows us to look at complex rotor bearing systems experiencing nonlinear transients and displays the vast amount of results in an easily understood motion-picture format. A 10-minute, 16-millimeter, color, sound motion-picture supplement is available, on loan, that shows the test data and the computer-made motion picture.

CONCLUSIONS

An implicit method for integrating the equations of motion for a lumped-mass model of a rotor dynamic system was developed. The following conclusions were drawn:

1. The method was numerically stable for any time step.
2. An error estimate was available to control the size of the time step.
3. The computational time was proportional to the number of elements in the rotor dynamics model rather than to the cube of the number.
4. An example problem with 19 mass elements in the rotor dynamics model took 0.7 second of central processing unit time per time step an an IBM 360-67 computer in a time-sharing mode.

For the first time, this code allows the simulation of a complex rotor bearing system experiencing nonlinear transients and displays the vast amount of results in an easily understood motion-picture format.

Lewis Research Center,
National Aeronautics and Space Administration,
Cleveland, Ohio, September 19, 1979,
505-04.

REFERENCES

1. Childs, D. W.: A Rotor-Fixed Modal Simulation Model of Flexible Rotating Equipment. J. Eng. Ind., vol. 96, no. 2, May 1974, pp. 659-669.
2. Gunter, E. J.; et al.: Transient and Stability Analysis Using the Modal Method. UVA/528144/ME77/102, University of Virginia, 1977.
3. Shen, F. A.: Flexible Rotor Dynamics Analysis. (R-9252, Rocketdyne; NASA Contract NAS3-14422.) NASA CR-121276, 1973.

4. Kascak, A. F.: Stability of Numerical Integration Techniques for Transient Rotor Dynamics. NASA TP-1092, 1977.
5. Gear, C. W.: Numerical Initial Value Problems in Ordinary Differential Equations. Prentice-Hall, Inc., 1971.
6. Barrett, L. E.; and Gunter, E. J.: Steady-State and Transient Analysis of a Squeeze Film Damper Bearing for Rotor Stability. NASA CR-2548, 1975.
7. Kirk, R. G.; and Gunter, E. J.: Nonlinear Transient Analysis of Multi-Mass Flexible Rotors - Theory and Applications. NASA CR-2300, 1973.
8. Cunningham, R. E.; Fleming, D. P.; and Gunter, E. J.: Design of a Squeeze-Film Damper for a Multi-Mass Flexible Rotor. ASME Trans. J. Eng. Ind., vol. 97, no. 4, Nov. 1975, pp. 1383-1389.

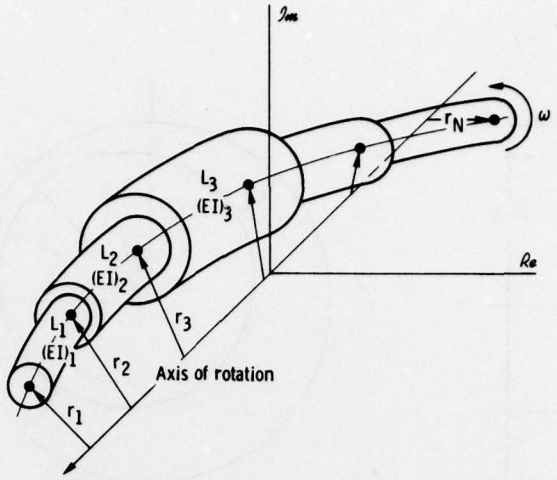

Figure 1. - Model of shaft showing complex number representation of radial displacements.

$$
0 = \begin{bmatrix} \Sigma F_{x_1} \\ \Sigma F_{y_1} \\ \Sigma G_{x_1} \\ \Sigma G_{y_1} \end{bmatrix} + \begin{bmatrix} B_1 & C_1 & 0 & \cdot & 0 \\ A_2 & B_2 & C_2 & \cdot & \cdot \\ 0 & \cdot & \cdot & \cdot & 0 \\ \cdot & \cdot & A_{N-1} & B_{N-1} & C_{N-1} \\ 0 & \cdot & 0 & A_N & B_N \end{bmatrix} \begin{bmatrix} u_{x_1} \\ u_{y_1} \\ u_{x_1'} \\ u_{y_1'} \\ \cdot \\ \cdot \\ \cdot \\ \cdot \\ u_{x_N} \\ u_{y_N} \\ u_{x_N'} \\ u_{y_N'} \end{bmatrix}
$$

Figure 2. - Newton-Raphson technique that leads to a linear set of block-tridiagonal equations.

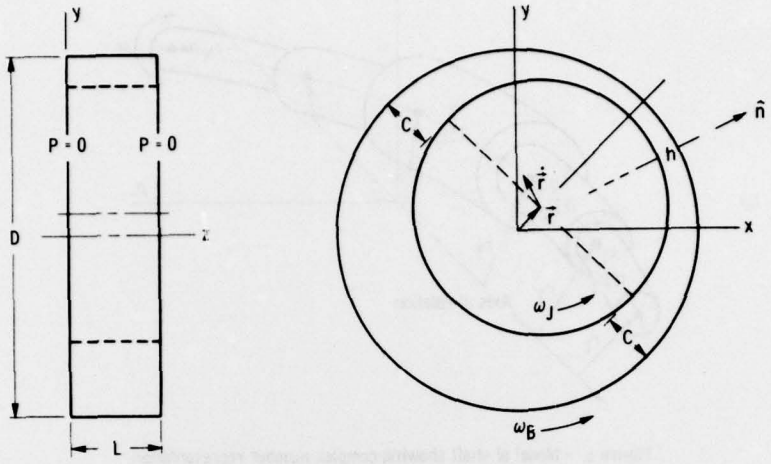

Figure 3. - Damper bearing geometry.

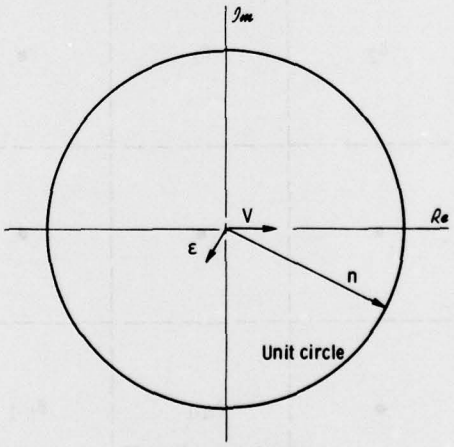

Figure 4. - Complex plane.

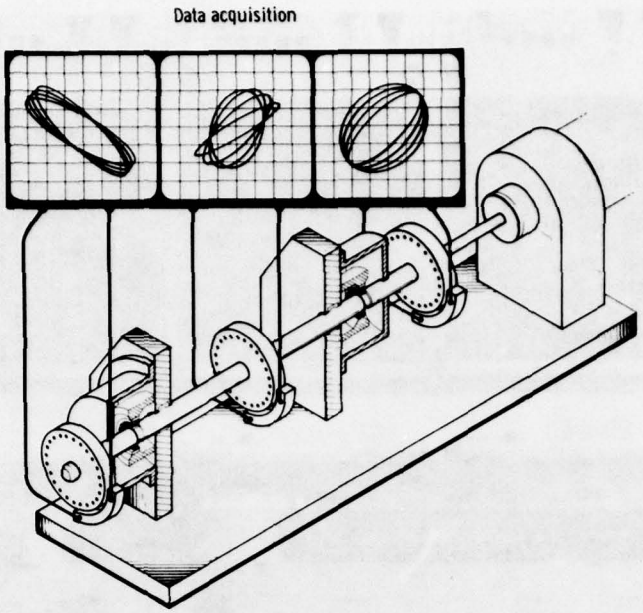

Figure 5. - Rotor bearing system used as example problem.

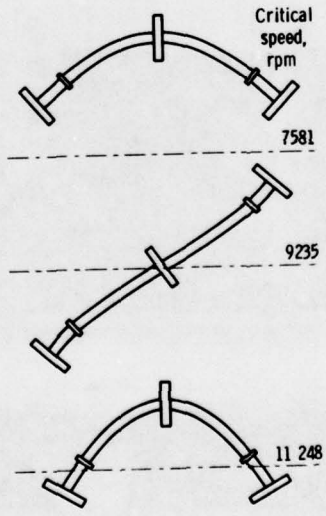

Figure 6. - Undamped critical speeds.

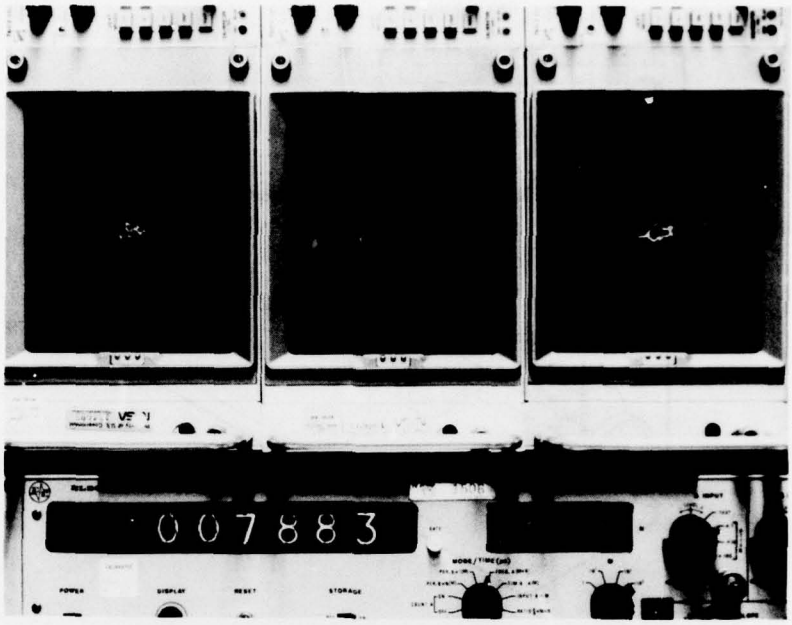

Figure 7. - Rotor passing through first critical speed.

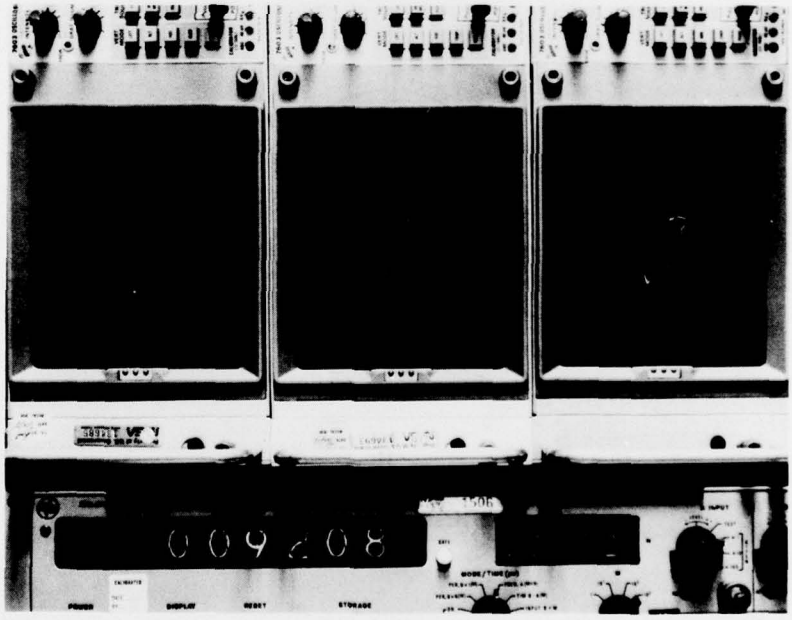

Figure 8. - Rotor passing through second critical speed.

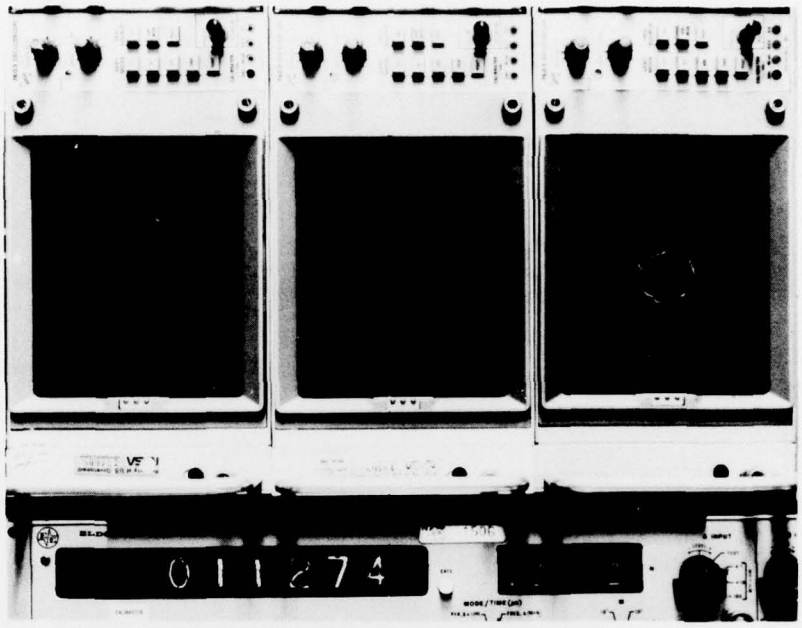

Figure 9. - Rotor passing through third critical speed.

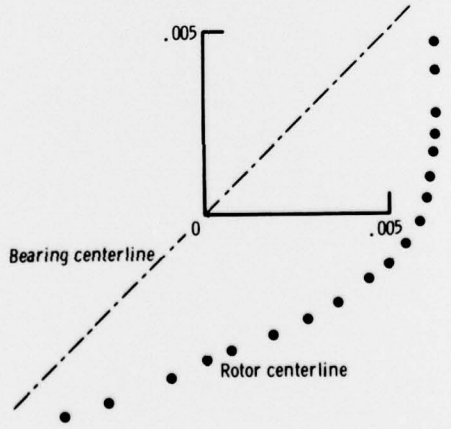

Figure 10. - Oblique view of rotor centerline as rotor passes through first critical speed.

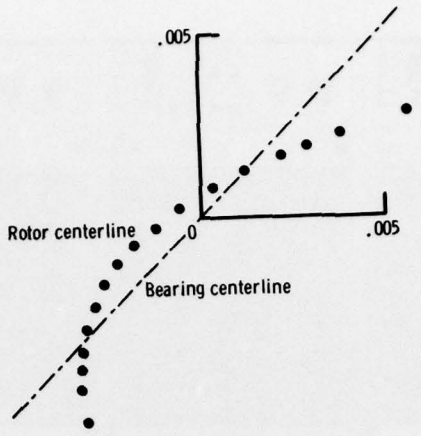

Figure 11. - Oblique view of rotor centerline as rotor passes through third critical speed.

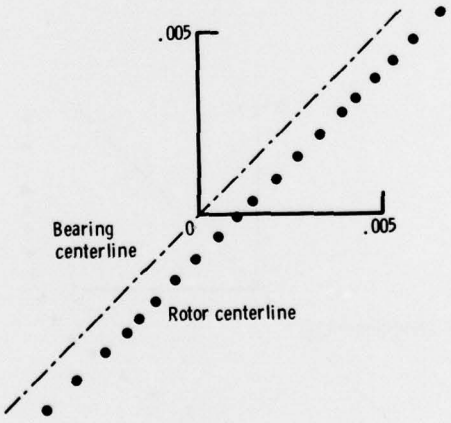

Figure 12. - Oblique view of rotor centerline at rotor speeds much greater than third critical.

1. Report No.	2. Government Accession No.	3. Recipient's Catalog No.
NASA TP-1597 USAAVRADCOM TR-79-42		

4. Title and Subtitle	5. Report Date
DIRECT INTEGRATION OF TRANSIENT ROTOR DYNAMICS.	January 1980
	6. Performing Organization Code

7. Author(s)	8. Performing Organization Report No.
Albert F. Kascak	E-101
	10. Work Unit No.
	505-04

9. Performing Organization Name and Address	11. Contract or Grant No.
NASA Lewis Research Center and AVRADCOM Research and Technology Laboratories Cleveland, Ohio 44135	
	13. Type of Report and Period Covered
12. Sponsoring Agency Name and Address National Aeronautics and Space Administration Washington, D.C. 20546 and U.S. Army Aviation Research and Development Command, St. Louis, Mo. 63166	Technical Paper
	14. Sponsoring Agency Code

15. Supplementary Notes

16. Abstract

An implicit method was developed for integrating the equations of motion for a lumped-mass model of a rotor dynamics system. As an aside, a closed-form solution to the short-bearing theory was also developed for a damper with arbitrary motion. The major conclusions are that the method is numerically stable and that the computation time is proportional to the number of elements in the rotor dynamics model rather than to the cube of the number. This computer code, for the first time, allows the simulation of a complex rotor bearing system experiencing nonlinear transient motion and displays the vast amount of results in an easily understood motion-picture format - a 10-minute, 16-millimeter, color, sound motion-picture supplement. An example problem with 19 mass elements in the rotor dynamics model took 0.7 second of central processing unit time per time step on an IBM 360-67 computer in a time-sharing mode.

17. Key Words (Suggested by Author(s))	18. Distribution Statement
Rotors Rotating shafts Numerical integration Numerical stability	Unclassified - unlimited STAR Category 07

19. Security Classif. (of this report)	20. Security Classif. (of this page)	21. No. of Pages	22. Price*
Unclassified	Unclassified	22	A03

* For sale by the National Technical Information Service, Springfield, Virginia 22161

NASA-Langley, 1980